CrossMark

ORIGINAL PAPER

Determination of 2,4-dichlorophenol in water samples using a chemiluminescence system consisting of graphene quantum dots, rhodamine B and cerium(IV) ion

Tooba Hallaj[1] · Mohammad Amjadi[1]

Abstract We report that the presence of graphene quantum dots (GQDs) causes an ~60-fold enhancement of the chemiluminescence (CL) caused by the reaction between rhodamine B (RhB) and Ce(IV) ion. A possible CL mechanism is established on the basis of fluorescence, CL and UV-vis spectra. It is suggested that the GQDs facilitate the oxidation of RhB and accelerate the generation of the CL emitting species, thus leading to stronger CL intensity. We further observed that 2,4-dichlorophenol at even trace levels exerts a diminishing effect on this CL system. This finding was exploited to design a CL method for determination of 2,4-dichlorophenol in the 0.1 to 5.0 μM concentration range, with a detection limit of 25 nM. The method was applied to the analysis of spiked real water and wastewater samples and gave satisfactory results.

Introduction

Graphene quantum dots (GQDs) are graphene fragments smaller than 100 nm which exhibit numerous unique physicochemical properties due to the pronounced quantum con-

✉ Mohammad Amjadi
amjadi@tabrizu.ac.ir

[1] Department of Analytical Chemistry, Faculty of Chemistry, University of Tabriz, Tabriz 5166616471, Iran

finement and edge effects. They have low cytotoxicity, excellent solubility, chemical inertia, stable photoluminescence and appropriate surface grafting property [1–3]. GQDs can also be used in chemiluminescence (CL) reactions. CL-based methods have been widely applied in the environmental analysis because of their high sensitivity, wide dynamic ranges, low detection limits, simplicity of instrumentation and short analysis time [4]. However, there are few reports on the CL studies of GQDs [5–7], though the application of other luminescent carbon nanomaterials in CL has been reported frequently. These nanomaterials often participate in a CL reaction as emitting species, after direct oxidation [8–15] or CL energy transfer [14–19], but their participation as catalysts has rarely been reported [7, 20, 21].

Chlorophenols are an important group of environmental pollutants which are concerned due to their toxicity and widespread uses. One of the most toxic chlorophenols listed in the Priority Pollutant List of the US Environmental Protection Agency, is 2,4-dichlorophenol (2,4-DCP). It is widely used as pesticide, herbicide, fungicide, molluscide, acaricide, bactericide, mold inhibitor and wood preservative. Other sources of 2,4-DCP in the environment include biodegradation of pesticides and herbicides such as 2,4-dichlorophenoxyacetic acid which often used on food crop and can be broken down to 2,4-DCP [22]. Therefore, monitoring of 2,4-DCP has appeared of great importance in environmental analysis. Various analytical methods including some CL-based methods have been reported [23–26].

In this work, we examined the catalytic effect of GQDs on the rhodamine B (RhB)-Ce(IV) CL reaction. It was found that GQDs remarkably enhanced the CL emission of this reaction. Furthermore, we found that the CL intensity of this system diminished in the presence of trace amount of 2,4-DCP. Based on this effect, a sensitive CL method

🖄 Springer

has been established for the determination of 2,4-DCP in water and wastewater samples.

Experimental

Apparatus

The CL signals were monitored by LUMAT LB 9507 chemiluminometer (Berthold; www.berthold.com). The luminometer was equipped with an automatic injector working on the basis of JET injection technology® and being used for injecting the oxidant. CL spectrum was recorded by RF-540 spectrofluorimeter (Shimadzu, Japan, www.shimadzu.com) using flow mode with the excitation light source being turned off. The fluorescence spectra were also recorded by the same instrument under normal conditions. UV–vis spectra were recorded by an AvaSpec-2048 Spectrophotometer (Avantes; www.avantes.com). The size and shape of GQDs were characterized by transmission electron microscopy (TEM, EM 900, Zeiss, Germany).

Reagents

All reagents were of analytical reagent grade. Doubly distilled deionized water (obtained from Ghazi Serum Co. Tabriz, Iran) was used throughout the experiment. Citric acid monohydrate, sodium hydroxide, RhB, Cerium(IV) sulfate and sulfuric acid were all obtained from Merck (Darmstadt, Germany, www.merck-chemicals.com). Chlorophenols was purchased from Sigma-Aldrich (www.sigmaaldrich.com). Ce(IV) solution (0.01 M) was prepared in 0.2 M H_2SO_4.

Synthesis of GQDs

GQDs were synthesized by pyrolyzing citric acid according to the literature [27]. Briefly, 2.0 g of citric acid was put into a beaker and heated to 200 °C by a heating mantle until the citric acid changed to an orange liquid. Then, for preparing GQDs, 100 mL of 10 mg mL^{-1} NaOH solution was added into the liquid dropwise with continuous, vigorous stirring. The obtained GQD solution was purified by dialysis (MW = 2000) against deionized water for 12 h and its concentration was calculated according to the concentration of carbon atom in the carbon source. The fluorescence spectra (Fig. S1, Electronic Supplementary Material, ESM), recorded every two weeks, confirmed that the prepared GQD solution was stable for at least one month in the refrigerator.

General procedure for CL monitoring

CL assay was carried out in a 3 mL tube, in the batch condition with the automatic injection system, which provides high speed and repeatable mixing of the reagents. An amount of 100 μL of RhB (1.0×10^{-4} M) and 150 μL of diluted prepared GQDs (0.68 mg mL^{-1}) were added into the cell. Then an appropriate volume of sample or standard solution was added and the final volume was reached to 900 μL with distilled water. After injection of 100 μL of 0.01 M Ce(IV) by the automatic injector, monitoring of CL signal versus time was started automatically. Maximum CL intensity was used as the analytical signal.
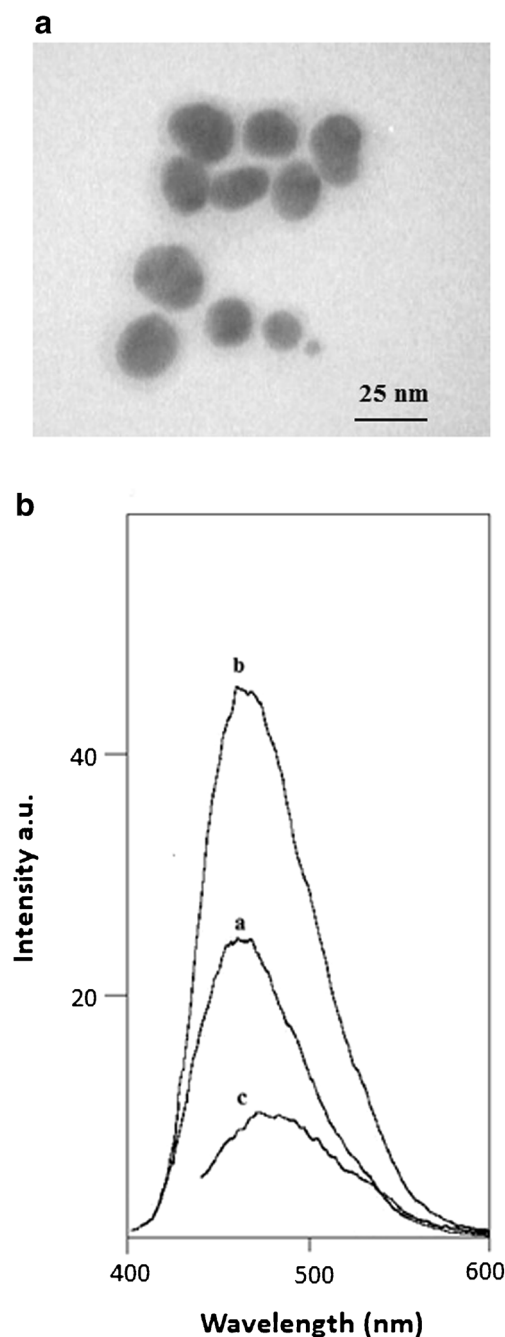

Fig. 1 **a** TEM image and **b** fluorescence spectra for GQDs excited at 375–425 nm wavelength range, with increments of 25 nm

Preparation procedure for real samples

Well and river water samples were obtained from environs of Tabriz (Iran). Wastewater sample was obtained from effluent of a pesticide factory (Karaj, Iran). In order to remove particulate materials, the wastewater was filtered with a 0.45 μm filter before analysis. No pretreatment was necessary for water samples. An appropriate volume of real samples was taken for analysis according to the general procedure.

Results and discussion

Characterization of GQDs

A simple carbonization was used for synthesis of GQDs. This is a well-established method, which appeared in many reports [27–31]. Citric acid is also used for preparation of carbon dots but with a different method, usually a hydrothermal procedure using some capping agent. The TEM image (Fig. 1a) shows that synthesized GQDs are nearly monodisperse nanoparticles with size distribution in the range of 20 ± 5 nm. As shown in Fig. 1b, the prepared GQDs revealed an excitation-independent fluorescence feature. When the excitation wavelength changes from 375 to 425 nm, the fluorescence spectra are almost invariable. This could be explained by the uniformity both in the size and the surface state of those sp^2 clusters contained in GQDs (vide infra) which was responsible for the fluorescence of GQDs [27]. The maximum emission of ~470 nm was obtained with an excitation wavelength of 400 nm.

In order to examine the functional groups of the prepared GQDs, more characterization including FTIR, XPS and Raman spectroscopy were carried out, and their results were given in the supplementary file (Fig. S2-S4, ESM). As demonstrated by FTIR and XPS spectra (Fig. S3, ESM), the prepared GQDs
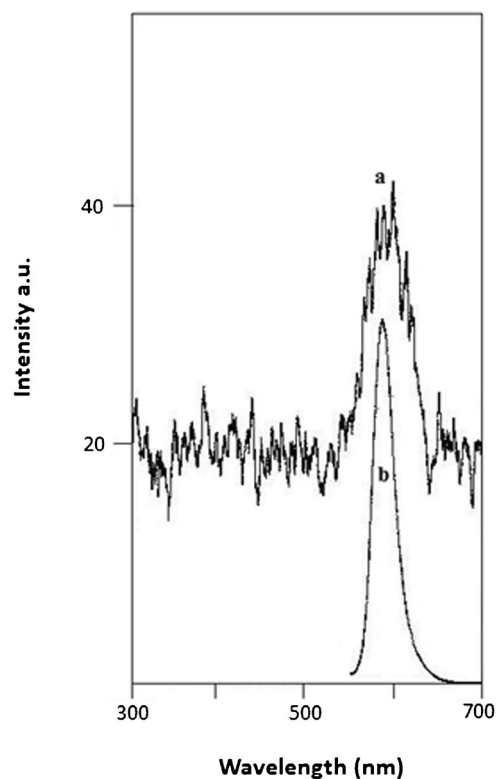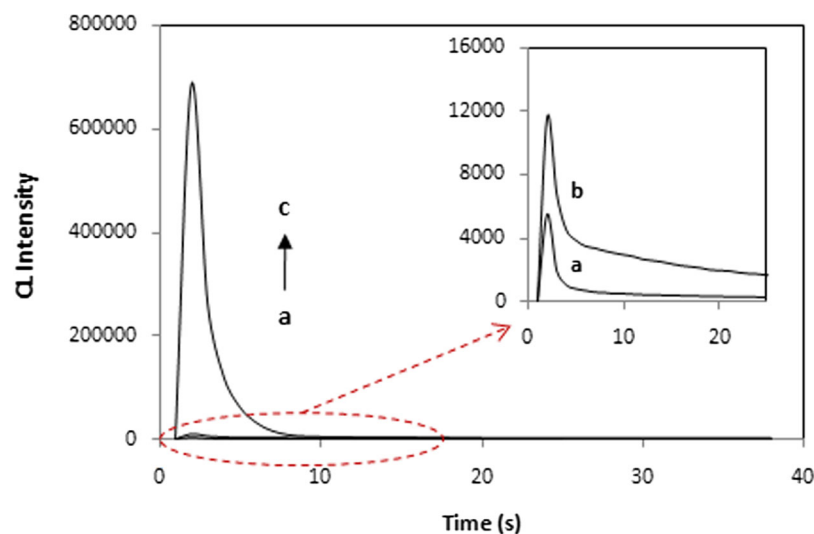

Fig. 3 **a** CL spectrum of RhB-Ce(IV)-GQDs system, obtained with continuous flow of reagents: GQD solution and RhB (2×10^{-5} M) in one line and Ce(IV) (2×10^{-3} M) and H$_2$SO$_4$ (0.04 M) in other line; **b** fluorescence spectrum of RhB, at $\lambda_{ex} = 500$ nm

contain C–O, C = C and C = O groups. XPS spectra showed a C1s peak at 284.8 eV and O1 speak at 533.0 eV (Fig. S3a, ESM). High-resolution XPS spectra of C1s (Fig. S3b, ESM) and O1s (Fig. S3c, ESM) regions revealed the presence of above mentioned functional groups on GQDs. Moreover, in Raman spectrum (Fig. S4, ESM), two characteristic peaks around 1370 and 1550 cm^{-1}, corresponding to the D and G band of graphene, respectively, were appeared.

Fig. 2 Kinetic curve for **a** GQD-Ce(IV), **b** RhB-Ce(IV) and **c** RhB-Ce(IV)-GQDs CL reactions. Conditions: RhB, 1.0×10^{-5} M, Ce(IV), 1.0×10^{-3} M, H$_2$SO$_4$, 0.02 M, GQDs, 0.10 mg mL^{-1}

Enhancement of CL intensity by GQDs

The enhancement effect of GQDs on the RhB-Ce(IV) CL reaction was investigated. Our studies indicated that a great enhancement (about 60-fold) in CL occurred when a small volume of GQD solution was added to this reaction (Fig. 2). Although GQDs were purified by dialysis, a control experiment with the reagents used for the preparation of GQDs (the mixture of citric acid and NaOH) was carried out. It was found that this solution had no contribution to the enhancement effect. Furthermore, 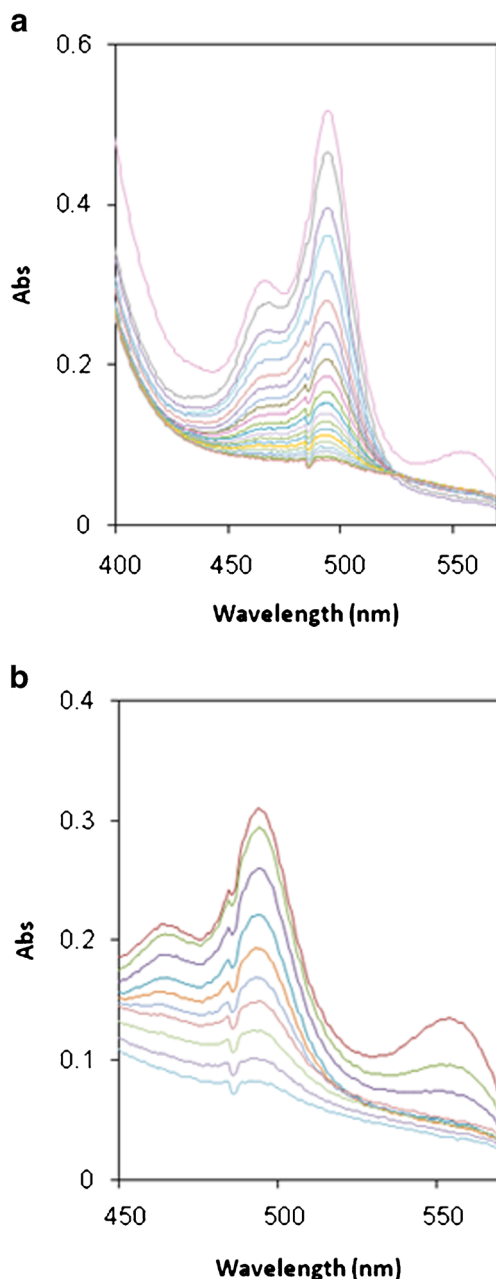direct reaction of Ce(IV) with GQDs was examined. As can be seen from Fig. 2a, a weak CL is produced by this reaction but in the presence of both Ce(IV) and RhB, the CL intensity is much more remarkable. The kinetic profiles of CL reaction in the absence and presence of GQDs (Fig. 2b,c) showed that the CL reaction was very fast and the CL intensity reached a maximum value within 1 s after injection of the oxidant solution.

Possible CL reaction mechanism

GQDs can participate in a CL reaction as emitters or catalysts. To determine their role in the present CL reaction, we recorded the CL emission spectrum of RhB- Ce(IV)-GQDs system using a spectrofluorometer in flow mode. The obtained CL spectrum (Fig. 3a) exhibited an emission band in the range of 500–700 nm with a peak at ~590 nm. This CL spectrum is comparable with the RhB fluorescence spectrum (Fig. 3b). This result indicates that in contrast to our previous works [5, 6], GQDs do not act as emitting species in the present system and the CL emission may be reasonably attributed to the excited RhB.

Previously it has been reported that direct oxidation of RhB by some oxidant such as Ce(IV) [32, 33] and KMnO$_4$ [34, 35] produces CL emission. It has been assumed that an intermediate is formed during the reaction process, which shows an absorption peak at about 490 nm. This peak decreases rapidly due to a subsequent redox reaction, involving production of the excited radical emitters.

In order to investigate the enhancing mechanism of GQDs on the CL reaction, we also recorded the fast-scan UV–Vis spectra of RhB and RhB–GQDs at various time intervals after addition of Ce(IV). According to the results (Fig 4a), instantly after addition of Ce(IV) to RhB solution a new peak appeared at around 490 nm. The intensity of this peak decreased with time and disappeared after about 45 s. This peak can be attributed to the intermediate product of the RhB and Ce(IV) reaction ([RhB-Ce]) which is previously introduced in the literatures as a precursor of excited radical emitter (RhB^{-*}) [33, 34] The UV–Vis spectra of Ce(IV)–RhB–GQDs (Fig 4b) exhibited a similar behavior. But, the intensity of intermediate peak at

Fig. 4 UV-Vis spectra of **a** RhB-Ce(IV) recorded at 2 s intervals and **b** RhB- Ce(IV)-GQDs recorded at 0.25 s intervals after addition of Ce(IV). RhB, 10^{-5} M, GQDs, 0.10 mg mL^{-1}, Ce (IV), 10^{-3} M, H$_2$SO$_4$ 0.02 M
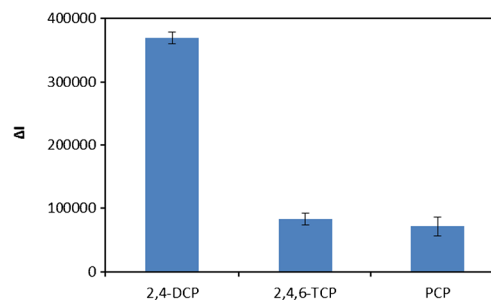
Fig. 5 Effect of chlorophenols on the RhB-Ce(IV)-GQDs CL systems. Conditions: RhB, 1.0×10^{-5} M, Ce(IV), 1.0×10^{-3} M, H$_2$SO$_4$, 0.02 M, GQDs, 0.10 mg mL^{-1}, Cholorophenols, 5 μM

490 nm decreased much more rapidly with time and disappeared after about 3 s. These results indicate that in the presence of GQDs the rate of the reaction involving the production of emitter (RhB$^{-\bullet*}$) from the mentioned intermediate ([RhB-Ce]) considerably increases. This is probably due to an electrostatic interaction between GQDs, which known to have the negative surface charge [28, 29], and cationic RhB molecules. Such an attractive interaction leads to an increase in the local concentration of RhB, which in turn facilitates the electron transfer from RhB to the Ce(IV) and accelerates the generation of emitter, leading to a higher CL intensity. The CL spectrum of RhB-Ce(IV) in the absence of GQDs could not be obtained due to its low intensity. However, an emission wavelength of 425 nm (attributed to RhB$^{-\bullet*}$) has been reported for this reaction [32]. By accepting this value, an overlap between the absorption band of RhB and the emission band of RhB$^{-\bullet*}$ can be assumed. Therefore, an energy transfer may occur from this anion radical to RhB.

Based on the mentioned phenomena, the enhanced CL mechanism can be summarized as follows:

$$RhB + Ce\,(IV) \rightarrow [RhB-Ce]$$

$$[RhB-Ce] \overset{GQDs}{\rightarrow} RhB^{-\bullet*}$$

$$RhB^{-\bullet*} + RhB \rightarrow RhB^* + RhB^-$$

$$RhB^* \rightarrow RhB + h\upsilon\,(590\ nm)$$
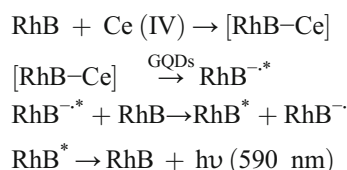
Optimization of chemical conditions

In order to obtain the maximum sensitivity for the introduced reaction, the effects of several variables such as concentration of RhB, Ce(IV), H_2SO_4 and GQDs on the CL intensity were investigated.

The effect of RhB concentration on the CL intensity was examined in the range of 1.0×10^{-6} M to 2.0×10^{-4} M. According to Fig. S5a (ESM), the CL response increased by increasing RhB concentration up to 1.0×10^{-5} M probably due to producing more exited-state RhB. So, 1.0×10^{-5} mol L^{-1} RhB was chosen as the optimum value for subsequent experiments.

Table 2 Results for the determination of 2,4-DCP in real samples

Sample	Added (μM)	Found (μM) [a]	Recovery (%)	t-Statistic [b]
Wastewater	0.0	48.8 ± 1.0	-	-
	50	98.3 ± 2.2	98.9 ± 4.5	0.38
	100	148.7 ± 3.1	99.8 ± 3.1	0.06
River water	0.0	ND [c]	-	-
	5	5.1 ± 0.2	101.8 ± 3.9	0.78
	10	9.5 ± 0.2	95.0 ± 2.4	4.04
Well water	0.0	ND [c]	-	-
	5	4.8 ± 0.1	96.0 ± 3.0	2.33
	10	9.7 ± 0.3	97.5 ± 3.0	1.48

[a] Mean of three determinations ± standard deviation
[b] t-Critical = 4.3 for $n = 2$, $P = 0.05$
[c] Not detected

The effect of the concentration of GQD solution in the range of 0.017–0.27 mg mL^{-1} on the CL intensity was also examined (Fig. S5b, ESM). The CL intensity is increased by increasing the GQD concentration until 0.10 mg mL^{-1}. However, at higher concentrations the excess GQDs may compete with RhB for Ce(IV) and causes a decrease in the CL intensity.

In order to study the effect of Ce(IV) concentration, solutions with different concentration of Ce(SO$_4$)$_2$.4H$_2$O were prepared over the range of 2.5×10^{-4} to 2.5×10^{-3} M. According to the results (Fig. S5c, ESM), maximum CL response was obtained for 1.0×10^{-3} M Ce(IV). At lower concentrations the number of excited intermediates is decreased and the response is diminished. Finally, the influence of sulfuric acid concentration in Ce(IV) solution on the CL signal was also investigated. As shown in Fig. S5d (ESM), the CL signal reached a maximum value at 0.02 M sulfuric acid, so this concentration was used for further work.

Analytical application of the CL system

In order to examine the analytical applicability of the RhB-GQDs-Ce(IV) CL system, the effect of some important chlorophenols including 2,4-DCP, 2,4,6-tricholorophenol (2,4,6-TCP) and pentachlorophenol (PCP) on the CL reaction was examined (Fig. 5). All of these compounds decreased

Table 1 Comparison of the developed method for the determination of 2,4-DCP with some previously published CL methods

CL system	Linear range (μM)	Detection limit (nM)	Ref
Luminol-NaOH-AuNPs	0.6–122	80	[23]
CdTe phototransformed 2,4-DCP-NBC [a]	0.36–36	130	[24]
Fluorescein phototransformed 2,4-DCP-NBC	-	150	[25]
Luminol-KMnO$_4$	0.6–122	110	[26]
RhB-Ce(IV)-GQDs	0.1–5.0	25	This work

[a] N-bromosuccinimide

the CL intensity but 2,4-DCP had much more remarkable influence than others. 2,4-DCP has a reducing property and can compete with RhB for Ce(IV) which leads to a decrease in the CL emission intensity. Based on this effect, we have designed a sensitive method for the determination of 2,4-DCP. Under the optimum conditions mentioned above, the analytical figures of merit for determination of 2,4-DCP were obtained. The CL response was found to be linear in the concentration range from 0.1 to 5.0 μM with a detection limit (3 s) of 25 nM (Fig. S6a, ESM). The regression equation was $\Delta I = 70922C + 4958$, $R^2 = 0.9958$, where $\Delta I = I_0-I$ is the difference between the CL intensity in the absence of 2,4-DCP (I_0) and in its presence (I), and C is concentration of 2,4-DCP in μM (Fig. S6b, ESM). The relative standard deviation (RSD) was obtained to be 2.6 % for five replicate determinations of 1.0 μM 2,4-DCP. The results indicate that this CL system has a good linearity, relatively high sensitivity and suitable precision. Comparison between the developed method and some other reported CL methods for the 2,4-DCP quantification is shown in Table 1. As can be seen, the detection limit of the developed method is much better than other CL methods. Moreover, our method is much simpler and faster than the methods involving phtotransformation [24, 25] and molecularly imprinted polymer based-extraction [25].

Study of interferences

The interfering effect of some species commonly found in environmental water samples, on the determination of 1.0 μM of 2,4-DCP was investigated. The tolerable concentration ratios for interferences in relative error of <5 % were over 15,000 for Na^+, K^+, NO_3^- and Cl^-, 4500 for Ba^{2+}, 3700 for Ca^{2+}, 1500 for Cu^{2+}, 1300 for Mn^{2+}, 1000 for Mg^2 and SO_4^{2-}, 400 for Co^{2+}, Fe^{2+} and Zn^{2+}, 300 for Pb^{2+}, 100 for Cr^{3+}, 25 for Hg^{2+}, 10 for bisphenol A, 1-naphthol, hydroquinone and uric acid, 5 for pentachlorophenol, trichlorophenol and 2-nitrophenol and 1 for resorcinol. Furthermore, humic acid did not interfere up to 20 mg L^{-1}. The corresponding data for interferences were given in supplementary file (Table S1, ESM). As can be seen, the most important interfering species in this determination is resorcinol, but the possibility of its co-occurrence with 2,4-DCP is low because of their different application areas. Therefore, the developed method is applicable for analysis of real water and wastewater samples.

Analysis of real samples

The method was applied for the determination of 2,4-DCP in real water and wastewater samples. In order to confirm the accuracy of the method, known quantities of 2,4-DCP were added to the samples and then they were prepared and analyzed according to the general procedure. The obtained results are shown in Table 2. Statistical analysis of these results using Student t-test showed that there are no significant differences between the added and found values.

Conclusion

We demonstrated here that GQDs can dramatically enhance the CL intensity of RhB-Ce(IV) reaction. The RhB-Ce(IV)-GQDs reaction was then introduced as a useful CL system and the possible CL mechanism of this reaction was studied. It was suggested that GQDs may act as catalysts to facilitate the oxidation of RhB leading to higher CL intensity. In addition, it was found that even trace levels of 2,4-DCP reduce the CL intensity of RhB-Ce(IV)-GQDs system. On the basis of this fact, we established a sensitive CL method for the determination of 2,4-DCP. The designed method was exploited to the detection of 2,4-DCP in water and wastewater samples with satisfactory results.

References

1. Zheng XT, Ananthanarayanan A, Luo KQ, Chen P (2015) Glowing graphene quantum dots and carbon dots: properties, syntheses, and biological applications. Small 11:1620–1636
2. Li L, Wu G, Yang G, Peng J, Zhao J, Zhu J-J (2013) Focusing on luminescent graphene quantum dots: current status and future perspectives. Nanoscale 5(3):4015–4039
3. Lin L, Rong M, Luo F, Chen D, Wang Y, Chen X (2014) Luminescent graphene quantum dots as new fluorescent materials for environmental and biological applications. TrAC Trends Anal Chem 54:83–102
4. Ocaña-González JA, Ramos-Payán M, Fernández-Torres R, Villar Navarro M, Bello-López MÁ (2014) Application of chemiluminescence in the analysis of wastewaters – a review. Talanta 122:214–222
5. Amjadi M, Manzoori JL, Hallaj T (2014) Chemiluminescence of graphene quantum dots and its application to the determination of uric acid. J Lumin 153:73–78
6. Hallaj T, Amjadi M, Manzoori JL, Shokri R (2015) Chemiluminescence reaction of glucose-derived graphene quantum dots with hypochlorite, and its application to the determination of free chlorine. Microchim Acta 182:789–796
7. Hao M, Liu N, Ma Z (2013) A new luminol chemiluminescence sensor for glucose based on pH-dependent graphene oxide. Analyst 138:4393–4397
8. Dong Y, Dai R, Dong T, Chi Yand Chen G (2014) Photoluminescence, chemiluminescence and anodic electrochemiluminescence of hydrazide-modified graphene quantum dots. Nanoscale 6:11240–11245
9. Xue W, Lin Z, Chen H, Lu C, Lin J-M (2011) Enhancement of ultraweak chemiluminescence from reaction of hydrogen peroxide and bisulfite by water-soluble carbon nanodots. J Phys Chem C 115:21707–21714
10. Lin Z, Xue W, Chen H, Lin J-M (2012) Peroxynitrous-acid-induced chemiluminescence of fluorescent carbon dots for nitrite sensing. Anal Chem 83:8245–8251

11. Lin Z, Xue W, Chen H, Lin J-M (2011) Classical oxidant induced chemiluminescence of fluorescent carbon dots. Chem Commun 48: 1051–1053

12. Amjadi M, Manzoori JL, Hallaj T, Sorouraddin MH (2014) Direct chemiluminescence of carbon dots induced by potassium ferricyanide and its analytical application. Spectrochim Acta A 122:715–720

13. Teng P, Xie J, Long Y, Huang X, Zhu R, Wang X (2014) Chemiluminescence behavior of the carbon dots and the reduced state carbon dots. J Lumin 146:464–469

14. Amjadi M, Manzoori JL, Hallaj T, Sorouraddin MH (2014) Strong enhancement of the chemiluminescence of the cerium(IV)-thiosulfate reaction by carbon dots, and its application to the sensitive determination of dopamine. Microchim Acta 181:671–677

15. Jiang J, He Y, Li S, Cui H (2012) Amino acids as the source for producing carbon nanodots: microwave assisted one-step synthesis, intrinsic photoluminescence property and intense chemiluminescence enhancement. Chem Commun 48:9634–9636

16. Dou X, Lin Z, Chen H, Zheng Y, Lu C, Lin J-M (2013) Production of superoxide anion radicals as evidence for carbon nanodots acting as electron donors by the chemiluminescence method. Chem Commun 49(52):5871–5873

17. Shi J, Lu C, Yan D, Ma L (2013) High selectivity sensing of cobalt in HepG2 cells based on necklace model microenvironment-modulated carbon dot-improved chemiluminescence in Fenton-like system. Biosens Bioelectron 45:58–64

18. Zhou Y, Xing G, Chen H, Ogawa N, Lin J-M (2012) Carbon nanodots sensitized chemiluminescence on peroxomonosulfate–sulfite–hydrochloric acid system and its analytical applications. Talanta 99:471–477

19. Amjadi M, Manzoori JL, Hallaj T (2015) A novel chemiluminescence method for determination of bisphenol abased on the carbon dot-enhanced HCO^-_3–H_2O_2 system. J Lumin 158:160–164

20. Wang DM, Gao MX, Gao PF, Yang H, Huang CZ (2013) Carbon nanodots-catalyzed chemiluminescence of luminol: a singlet oxygen-induced mechanism. J Phys Chem C 117:19219–19225

21. Lin Z, Dou X, Li H, Chen Q, Lin J-M (2014) Silicon-hybrid carbon dots strongly enhance the chemiluminescence of luminol. Microchim Acta 181:805–811

22. Olaniran AO, Igbinosa EO (2011) Chlorophenols and other related derivatives of environmental concern: properties, distribution and microbial degradation processes. Chemosphere 83:1297–1306

23. Feng Q, Li H, Zhang Z, Lin J-M (2011) Gold nanoparticles for enhanced chemiluminescence and determination of 2,4-dichlorophenol in environmental water samples. Analyst 136:2156–2160

24. Wu H, Ding Z, Peng M, Song Q (2012) Quantum dot induced phototransformation of 2,4-dichlorophenol, and its subsequent chemiluminescence reaction. Microchim Acta 178:203–210

25. Zhang J, Song Q, Hu X, Zhang E, Gao H (2008) Dye-sensitized phototransformation of chlorophenols and their subsequent chemiluminescence reactions. J Lumin 128:1880–1885

26. Feng Q-Z, Zhao L-X, Yan W, Ji F, Wei Y-L, Lin J-M (2008) Molecularly imprinted solid-phase extraction and flow-injection chemiluminescence for trace analysis of 2,4-dichlorophenol in water samples. Anal Bioanal Chem 391:1073–1079

27. Dong Y, Shao J, Chen C, Li H, Wang R, Chi Y (2012) Blue luminescent graphene quantum dots and graphene oxide prepared by tuning the carbonization degree of citric acid. Carbon 50: 4738–4743

28. Dong Y, Li G, ZhouN WR, Chi Y, Chen G (2012) Graphene quantum dot as a green and facile sensor for free chlorine in drinking water. Anal Chem 84:8378–8382

29. He Y, Wang X, SunJ JS, Chen H, Gao F, Wang L (2014) Fluorescent blood glucose monitor by hemin-functionalized graphene quantum dots based sensing system. Anal Chim Acta 810:71–78

30. He Y, Sun J, Feng D, Chen H, Gao F, Wang L (2015) Graphene quantum dots: highly active bifunctional nanoprobes for nonenzymatic photoluminescence detection of hydroquinone. Biosens Bioelectron 74:418–422

31. Wu Z, Li W, Chen J, Yu C (2014) A graphene quantum dot-based method for the highly sensitive and selective fluorescence turn on detection of biothiols. Talanta 119:538–543

32. Ma Y, Jin X, Zhou M, Zhang Z, Teng X, Chen H (2003) Chemiluminescence behavior based on oxidation reaction of rhodamine B with cerium (IV) in sulfuric acid medium. Anal Chim Acta 489:173–181

33. Hasanin THA, Tsunemine Y, Tsukahara S, Okamoto Y, Fujiwara T (2011) Chemiluminescence from an oxidation reaction of rhodamine B with cerium (IV) in a reversed micellar medium of cetyltrimethylammonium chloride in 1-hexanol–cyclohexane/water. Anal Sci 27:297–304

34. Hassanzadeh J, Amjadi M, Manzoori JL, Sorouraddin MH (2013) Gold nanorods-enhanced rhodamine B-permanganate chemiluminescence and its analytical application. Spectrochim Acta A 107: 296–302

35. Amjadi M, Hassanzadeh J, Manzoori JL (2014) Determination of cyanide using a chemiluminescence system composed of permanganate, rhodamine B, and gold nanoparticles. Microchim Acta 181: 1851–1856